Electronic structure of small iron clusters

Keeyung Lee, Joseph Callaway, and S. Dhar
Department of Physics and Astronomy, Louisiana State University, Baton Rouge, Louisiana 70803-4001
(Received 12 March 1984)

We report calculations of energy levels and the charge and spin densities for small free (not embedded) clusters of iron atoms. Our method uses spin-density-functional theory in the local approximation. Single-particle functions are expanded in a basis set of symmetrized linear combinations of Gaussian orbitals. Matrix elements of the electrostatic potential are computed with the aid of a fit to the electron density, again with the use of symmetrized combinations of Gaussian orbitals. The matrix elements of the exchange-correlation potential are evaluated by direct numerical integration using a grid developed for this purpose. The clusters considered are Fe_7, Fe_9, and Fe_{15}. Our results are compared with those obtained by other calculational procedures. The ionization potential of the Fe_9 cluster is determined by a transition-state calculation and is compared with experiment.

I. INTRODUCTION

The study of the electronic structure of small atomic clusters has become of considerable interest. Such clusters are interesting both for themselves and as models for problems in solid-state physics involving the self-consistent treatment of impurities, local excitations, and even surfaces.

This paper reports that results of calculations of electron energy levels and charge and spin densities in small iron clusters. The clusters are free, that is, the problem of embedding a cluster in a solid so that the results will be representative of the solid is not addressed here. We consider specifically Fe_7, Fe_9, and Fe_{15} clusters in cubic geometries. The results are compared with those obtained by other authors. The ionization potential of Fe_9 is computed and compared with experiment.

Although a detailed review of methods for cluster calculations has not (so for as we know) yet appeared, the essential characteristics of the procedures in current use are summarized by Delley and Ellis.[1] Our calculations are based on the local- (spin-) density approximation to density-functional theory. The single-particle Kohn-Sham equations[2] (including spin polarization), are solved variationally and self-consistently by expansion in a basis set of Gaussian orbitals, similar to the procedure followed in our methods of energy-band calculations.[3] This is an all-electron calculation. No frozen-core calculation is employed, and there is no approximation of the "muffin-tin" type.

However, the large number of two-electron integrals that are produced if the electrostatic interaction terms are treated in the most straightforward way has led us to adapt a procedure in which the charge density is fitted to a secondary expansion in symmetrized combinations of Gaussian orbitals. This approach was proposed by Sambe and Felton[4] and has been extended by other authors.[5] Some remarks on our fitting procedure are contained in Sec. II; full details may be found in Ref. 6. The same procedure could be employed to compute matrix elements of the exchange-correlation potential; however, because it is not easy to get an accurate fit to this quantity, we have decided to compute these matrix elements by direct numerical integration using a special three-dimensional grid, which is described in the Appendix. Additional discussion of our methods is given in Sec. II.

Previously, calculations for similar iron clusters (Fe_4, Fe_9, and Fe_{15}) have been reported by Yang *et al.*[7] These authors employed the $X\alpha$ scattered-wave method. A cluster density of states for Fe_{15} was generated by replacing the sharp cluster levels by a Gaussian of width parameter 0.2 eV. Yang *et al.* concluded that all of the major features of the bulk density of states were already present in the cluster density of states. Spin-density maps were generated which resembled those for bulk iron. Values of the contact hyperfine field agreed reasonably well with those for bulk iron.

Our results will be compared in detail with those of Yang *et al.* in Sec. III. It suffices for the moment to note that we agree with their conclusion that the density of states for the Fe_{15} cluster is remarkably similar to that for bulk metallic iron. However, we find (and describe briefly below) significant differences between cluster and bulk results for the spatial distribution of the spin density.

II. METHOD

The effective one-electron Hamiltonian for electrons of spin σ has the form, according to local-spin-density-functional theory,

$$H_\sigma = -\nabla^2 + 2\sum_\mu \frac{Z_\mu}{|\vec{r}-\vec{R}_\mu|} + 2\int \frac{\rho(\vec{r}\,')}{|\vec{r}-\vec{r}\,'|} d^3r' + V_{xc\sigma}(\vec{r}) \,. \tag{2.1}$$

Atomic units, with energies in rydbergs, are used throughout this paper. In Eq. (2.1), $\vec{R}_\mu$ designates the position of the μth atom, and Z_μ is the nuclear charge (in units of the proton charge). The quantity $V_{xc\sigma}$ is the

exchange-correlation potential for electrons of spin σ. Here, we take this to have the von Barth–Hedin[8] form as parametrized by Rajagopal *et al.*[9] In a general form, we have

$$V_{xc\sigma}=A(\rho)(\rho_\sigma/\rho)^{1/3}+B(\rho)\ , \tag{2.2}$$

in which ρ_σ is the spin density, and $A(\rho)$ and $B(\rho)$ are numerical functions of the density.

The eigenfunctions of H, denoted ψ_κ (for convenience, κ designates all quantum numbers, including the spin σ which are required to designate a single-particle function) are expanded in a set of basis functions χ_j,

$$\psi_\kappa=\sum_j C_{j\kappa}\chi_j\ . \tag{2.3}$$

The χ_j are, in general, not orthonormal. The familiar equation results,

$$\underline{H}\,\underline{C}=E\underline{S}\,\underline{C}\ , \tag{2.4}$$

where now $\underline{H}$ denotes the Hamiltonian and $\underline{S}$ the overlap matrix on the basis chosen. As $\underline{H}$ depends on $\underline{C}$, a self-consistent solution has to be found by iteration.

The basis functions χ_j used here are combinations of Gaussian orbitals which transform according to the various irreducible representations of the group of the cluster. In the present case, this is the cubic group. The elementary Gaussian orbitals used in this calculation were chosen to be those used by Wachters[10] in a calculation of energy levels and wave functions for the isolated iron atom. The basis includes $14s$, $9p$, and $5d$ functions. Although it is certainly possible to contract this basis, we do not do so, but instead consider all the basis functions to be independent. This procedure improves the accuracy of wave functions, particularly near a nucleus. When angular dependences are included there are 66 basis functions per atom, so that the use of independent Gaussians is practical only because of the high symmetry of the cluster. This allows us to reduce the size of the matrix-diagonalization problem since only functions of the same symmetry need be considered in constructing the submatrices of H and S which are actually diagonalized. The coefficients required to form the symmetrized combinations were obtained by standard group-theoretic rules and were provided to the program as data. The coefficients are listed in Ref. 6, which contains additional discussion of the use of symmetry to simplify our calculations.

The matrix elements of the Hamiltonian between primitive Gaussian functions on the various sites are related by symmetry in many cases. These transformation properties greatly simplify the construction of the Hamiltonian and overlap matrices.

As mentioned earlier, the number of two-electron integrals, which increases as the fourth power of the number of primitive Gaussians, is so large in the present case that we must make an auxiliary fitting of the charge density, as was originally introduced by Sambe and Felton.[4] This fitting may be done in either of two ways: by making a least-squares fit to the charge density or by a variational approach which requires that the fit should produce minimum errors in the electrostatic energy of the electron distribution.[5] The latter procedure was adopted in this calculation.

In this approach, we define

$$\tilde{\rho}(\vec{r})=\sum_i a_i f_i(\vec{r})\ , \tag{2.5}$$

where the f_i are a set of functions to be used for the fit, and require that

$$\delta(D-\lambda N)=0\ , \tag{2.6}$$

where

$$D=\frac{e^2}{2}\int\frac{[\rho(\vec{r})-\tilde{\rho}(\vec{r})][\rho(\vec{r}\,')-\tilde{\rho}(\vec{r}\,')]}{|\vec{r}-\vec{r}\,'|}d^3r\,d^3r' \tag{2.7}$$

and

$$N=\int\tilde{\rho}(r)d^3r\ .$$

N is the actual electron number in the system. The solution for the coefficients a can be written in the form

$$a_i=(\underline{S}^{-1})_{ij}\left[t_j+\left[\frac{N-n_k(\underline{S}^{-1})_{kl}t_l}{n_k(\underline{S}^{-1})_{kl}n_l}\right]n_j\right]\ , \tag{2.8}$$

in which

$$S_{ij}=\int\frac{f_i(\vec{r})f_j(\vec{r}\,')}{|\vec{r}-\vec{r}\,'|}d^3r\,d^3r'\ , \tag{2.9}$$

$$t_j=\int\frac{f_j(\vec{r})\rho(\vec{r}\,')}{|\vec{r}-\vec{r}\,'|}d^3r\,d^3r'\ , \tag{2.10}$$

and

$$n_j=\int f_j(\vec{r})d^3r\ . \tag{2.11}$$

A summation convention (repeated indices imply summation) has been employed in Eq. (2.7).

The basis used for fitting the charge density contained symmetrized combinations of s-type Gaussians (both $1s$ and $3s$—by the latter, we refer to functions of the form $r^2e^{-\alpha r^2}$) centered on each atomic site. The exponents of the $1s$ Gaussians were taken to be twice those of the corresponding functions used in the wave-function expansion, whereas those for the $3s$ Gaussians were taken to be twice those for the p-type wave-function basis. Altogether, a total of 23 basis functions for each atom was employed in the charge-density fitting. We experimented with the addition of symmetrized combinations of p-type Gaussians to the fitting basis, but did not find significant improvement. In our procedure, the essential quantities required in the evaluation of the t_j [Eq. (2.10)] and for the computation of the Hamiltonian matrix are

$$(\underline{M}^{(k)})_{ij}=\int\frac{\chi_i(\vec{r})\chi_j(\vec{r})}{|\vec{r}-\vec{r}\,'|}f_k(\vec{r}\,')d^3r\,d^3r'\ . \tag{2.12}$$

These quantities (and also the S_{ij} and n_j) need be computed only once. The integrals are evaluated analytically.

In spite of very considerable effort devoted to the charge-density fitting procedure, this subject seems to us to be the weakest part of our calculations. It appears that a fully satisfactory solution will not be obtained short of

computation of all relevant two-electron integrals.

Since the exchange-correlation potential is smaller than the Coulomb potential over most of the cluster, it is plausible that less (percentage) accuracy is required in the computation of its matrix elements. We have computed these quantities by direct numerical integration on a special three-dimensional "approximate-doubling" grid. Since this grid has not, to our knowledge, appeared in the literature, we discuss its construction, and the accuracy obtained for some test integrals, in the Appendix. It is worth mentioning here that, because of the cubic symmetry of V_{xc}, the numerical integral needs to be performed in only $\frac{1}{48}$th of the "volume" of the cluster, providing symmetrized basis functions are used. We believe that a grid of about 1300 points gives matrix elements accurate to a few percent, and that this level of accuracy is acceptable.

The iterative calculations leading to self-consistency were slow to converge. This problem, and proposed remedies, have been discussed by others.[11,12] Let us define a mixing factor λ such that the input density to the $(i+1)$th iterative stage is λ times the appropriate output from the ith stage plus $1-\lambda$ times that from the $(i-1)$th stage. Then the situation may be summarized by the statement that λ must be small ($\sim 5\%$) in order to avoid oscillatory divergence of the procedure. We found that the procedure discussed by Dederichs and Zeller[12] of alternating larger and smaller values of λ (in our case, one iteration with $\lambda=0.15$ followed by three with $\lambda=0.05$) to be helpful. When oscillations due to changes in level positions near the Fermi energy were encountered, it was useful to replace the actual Fermi step-function occupancy by a smooth function (thus introducing, in effect, an artificial temperature). After a number of iterations, the $T=0$ limit could then be taken.

III. RESULTS

Our first preliminary calculations were made for Fe_7 clusters at two different atomic spacings, $5.4a_0$ and $4.0a_0$. The atoms were arranged in an octahedral fashion. These calculations employed a different method of evaluating exchange matrix elements in which the difference between the exchange potential at each stage of iteration and that initially assumed was fit to an expansion in Kubic harmonics. Both clusters were found to be ferromagnetic with average moments of $3.7\mu_B$/atom for the $5.4a_0$ spacing, and $3.0\mu_B$/atom at the $4.0a_0$ spacing. Both moments are higher than observed in bulk metallic iron. This may be a consequence of the open structure assumed. The Kubic harmonic expansion was abandoned in further work (in favor of the grid mentioned previously) because of difficulties in treating changes in the exchange potential close to a nucleus.

We then considered an Fe_9 cluster comprising a center atom and eight neighbors in the position corresponding to those of the bcc lattice at the distance of $4.68a_0$, corresponding to the nearest-neighbor distance in bulk iron. Our results for the energy levels in this system are summarized in Table I and in Fig. 1. The average magnetic moment was found to be $2.89\mu_B$/atom, in good agreement

TABLE I. Comparison of properties of iron clusters (energies in eV).

	Fe_9		Fe_{15}		Bulk
	MS $X\alpha$	Present	MS $X\alpha$	Present	Ref. 15
$(n\uparrow-n\downarrow)/N$	2.89	2.89	2.67	2.93	2.16
Occupied s-band width					
($\uparrow$)	4.7	6.7[a]	6.2	7.7[a]	8.20[b]
($\downarrow$)	3.7	6.3[a]	5.4	7.2[a]	8.03[b]
Occupied d-band width					
($\uparrow$)	3.8[c]	3.8[d]	4.5[c]	4.4[c]	4.75[e]
($\downarrow$)	1.5[c]	2.8[d]	2.9[c]	3.3[c]	3.60[e]
Total d-band width					
($\uparrow$)	2.4[f]	(2.8)[g] 4.4[h]	(2.9)[i] 4.5[j]	4.7[j]	5.13[k]
($\downarrow$)	2.8[l]	4.0[h]	(4.3)[m] 4.5[n]	5.3[o]	6.12[k]
Range of exchange splitting (d)	1.8—3.2	0.7—3.1	1.2—3.2	1.0—2.7	1.1—2.2
Average exchange splitting (d)	2.7	2.3	2.5	2.4	
Exchange splitting (sp)	1.0[p]	0.4[p]	0.8[p]	0.5[p]	0.16—0.85

[a] ϵ_F-$1a_{1g}$. [e] ϵ_F-N_1. [i] $6t_{2g}$-$1e_g$. [m] $3e_u$-$1e_g$.
[b] ϵ_F-Γ_1. [f] $4t_{1u}$-$1e_g$. [j] $7t_{2g}$-$1e_g$. [n] $6e_g$-$1e_g$.
[c] ϵ_F-$1e_g$. [g] $3e_g$-$1t_{2g}$ [k] N_3-N_1. [o] $3t_{1g}$-$1e_g$.
[d] ϵ_F-$1t_{2g}$. [h] $5t_{2g}$-$1t_{2g}$. [l] $4t_{2g}$-$1e_g$. [p] $1a_{1g\uparrow}$-$1a_{1g\downarrow}$.

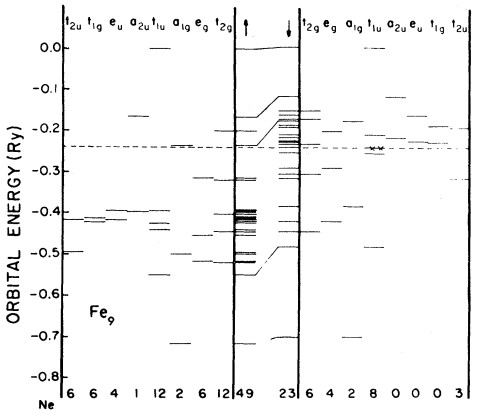

FIG. 1. Energy-level diagram for the Fe_9 cluster. The symmetries of levels and the occupancies (N_e) are given. The dashed line shows the position of the Fermi level at $t_{1u\downarrow}$, and the crosses indicate that it is occupied by two electrons.

with Ref. 7. Some numerical results for this system are compared with those of Ref. 7 and with bulk iron in Table I.

Because some experimental information is becoming available concerning the ionization potentials of small free-iron clusters,[13] we performed a transition-state calculation[14] to determine this quantity for the Fe_9 cluster. In this approach, the ionization potential is determined as the energy of the highest occupied state in a cluster in which this state has half an electron less than the normal occupancy. The calculation, which was also spin-polarized, gave 0.378 Ry (5.2 eV) for this quantity. Rohlfing *et al.*[13] state that the ionization potential for Fe_9 clusters is in the range from 5.3 to 5.6 eV. The agreement seems to be reasonable in view of the uncertain geometry of the experimental cluster.

We then proceeded to repeat the calculation for the Fe_{15} cluster (bcc geometry with $a=5.40$). Some of the numerical results are also presented in Table I where they are compared with those of Ref. 7. An energy-level diagram is shown in Fig. 2.

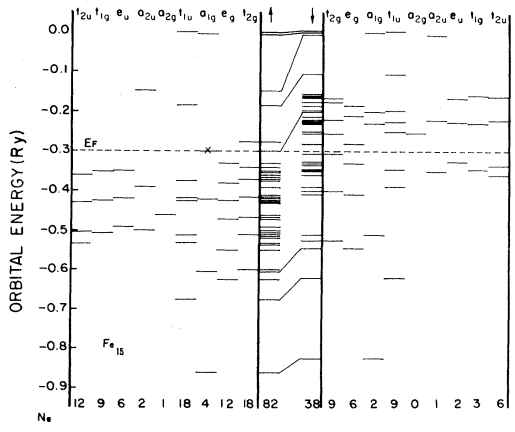

FIG. 2. Energy-level diagram for the Fe_{15} cluster.

Because one of the central questions in this area is the relation between cluster and bulk results, we have computed densities of states for both the Fe_9 and Fe_{15} clusters, which can be compared with results for bulk iron.[15] The quantity which involves the least ambiguity is the integrated density of states, $N(E)$, which is defined to be the number of states per atom with energies less than or equal to E. Specifically,

$$N(E)=\sum_i g_i \Theta(E-E_i)\ , \tag{3.1}$$

where g_i is the degeneracy of the state whose energy is E_i. This quantity is shown in Fig. 3 for the Fe_{15} cluster, for

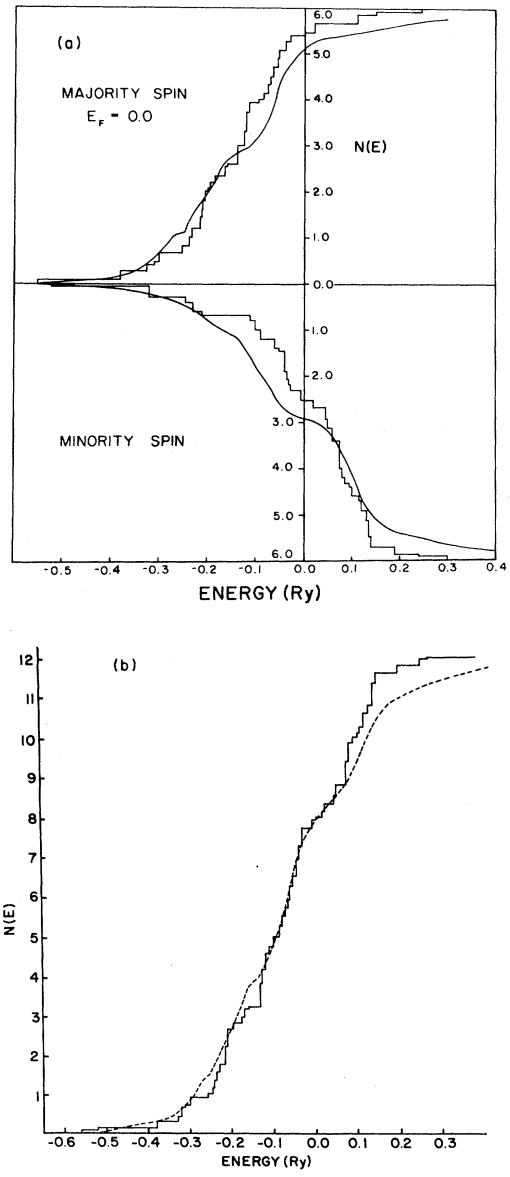

FIG. 3. (a) Integrated density of states per atom for Fe_{15} with majority and minority spins separated. The ordinate shows the number of states per atom. Results from the band calculation of Ref. 15 are presented, with the energies shifted so that the Fermi energies of the cluster and bulk coincide. (b) Integrated density of states per atom for Fe_{15} with spins combined.

both majority and minority spins. The results obtained from the band calculation of Ref. 15 are presented for comparison. The zero of energy has been taken as the Fermi energy for this purpose, and core levels are not included.

It will be seen that there is a substantial degree of general agreement between the cluster and bulk results in regard to the location of regions of relative flatness and or rapid increase. This indicates that this relatively small cluster already possesses an energy-level distribution which resembles that of bulk iron moderately well. This is consistent with the relatively small spatial extension d-electron wave functions.

The reasonable agreement obtained for the integrated density of states suggests that it is interesting to construct an approximate density of states. Here we have followed the procedure of Ref. 7 by using a Gaussian to broaden the cluster levels. Specifically,

$$G(E)=\frac{1}{N_A\sigma\sqrt{2\pi}}\sum_i g_i e^{-(E-E_i)^2/2\sigma^2}, \tag{3.2}$$

in which N_A is the number of atoms in the cluster. The choice of width parameter is essentially arbitrary. We used $\sigma=0.2$ eV, which is the value used in Ref. 7, and which gives reasonable results. It would be sensible to use a different width parameter for predominately s-p levels than for d-like levels, but we have not done this. The resulting density of states has been computed for majority and minority spins separately, and is shown for the Fe_9 cluster in Fig. 4 and for Fe_{15} in Figs. 5(a) and 5(b). The Fe_{15} results are compared with band results.

Our conclusion from these figures in regard to the energy-level distribution of predominately d states in these clusters is that as the size of the cluster increases, a very substantial resemblance between the general features of this distribution for the cluster and for the bulk metal develops. This conclusion is the same as that drawn by the authors of Ref. 7 and is in agreement with the view that the density of states depends only weakly on the boundary conditions imposed on the system.[16] In general, the agreement with bulk is much superior for the Fe_{15} cluster compared to the Fe_9 cluster, as one would expect. The agreement extends to some particular features of the density of states, as will be discussed below. However, we also find, in contrast to the results of Ref. 7 that the spin-density distribution is quite different from the bulk.

The most obvious feature of the level distribution is that we have a relatively narrow (in energy) distribution of levels formed primarily from d functions which is overlapped by a broader, less dense distribution of predominately s-p-like levels. This is, of course, characteristic of $3d$ transition-metal band structures in general. The widths of these s-p and d distributions, including the widths of occupied portions, are quite similar in the Fe_{15} cluster and the bulk, although they do not agree in detail. The present Fe_{15} values for bandwidths and exchange

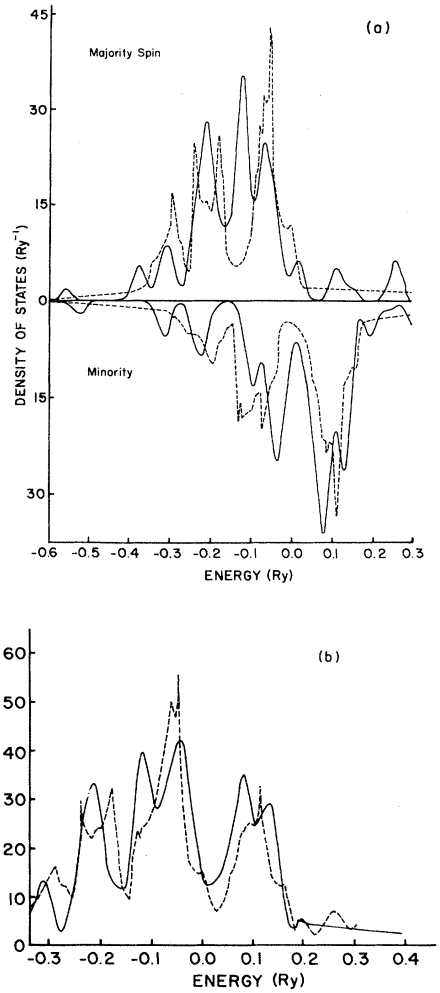

FIG. 5. (a) Cluster density of states per atom for Fe_{15} with majority and minority spins separated. Solid line, present calculation; dashed line, bulk iron from Ref. 15. (b) Cluster density of states per atom for Fe_{15} with spin states combined.

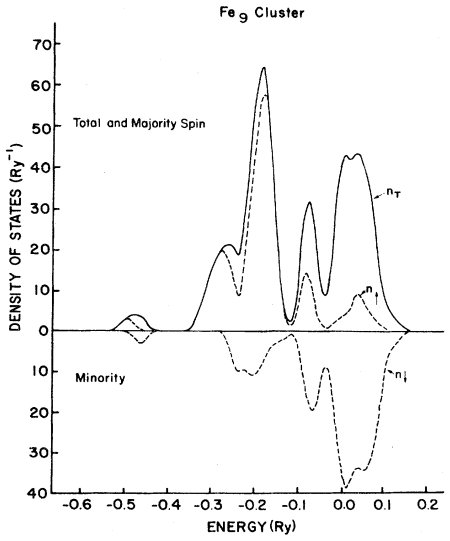

FIG. 4. Cluster density of states per atom for Fe_9.

splittings tend to be somewhat closer to the band-calculation results[15] as given in Table I than are the multiple-scattering $X\alpha$ (MS $X\alpha$) results (however, the band-calculation values in the footnotes of Table I refer to the von Barth—Hedin potential). In addition, note in Fig. 5(b) that the Fermi level for Fe_{15} is near a minimum of the density of states as in bulk iron, and that the peak structure on both sides of E_F in Fe_{15} is similar to the band result.

There is a major exception to this general agreement: The magnetic moment per atom in the case of Fe_{15} is much larger than the bulk value, and also larger than that obtained in the MS $X\alpha$ calculation. The spatial distribution of the spin density is also different. We have found a different pattern of positioning of some levels close to the Fermi energy which probably reflects differences in the band-calculation procedures. To see the cause of the difference, we can compare Fig. 2 with Fig. 6 of Ref. 7. In the present case, we find that there are no degeneracies at the Fermi energy; there are four occupied states with $a_{1g\uparrow}$ symmetry, six occupied doubly degenerate states with $e_{g\uparrow}$ symmetry, but only three occupied triply degenerate states with $t_{1u\downarrow}$ symmetry. Yang *et al.* have three electrons with $a_{1g\uparrow}$ symmetry and eleven (each) for the $e_{g\uparrow}$ and $t_{1u\downarrow}$ symmetries; the incomplete occupancies of these states results from a degeneracy at the Fermi energy. In our case the sixth $e_{g\uparrow}$ state is below E_F, as is the fourth $a_{1g\uparrow}$, while our fourth $t_{1u\downarrow}$ is above E_F. Thus we have two more majority-spin electrons in the cluster than was found by Yang *et al.* and we thus obtain a larger moment. It is difficult for us to understand the occurrence of the accidental degeneracy of the $e_{g\uparrow}$ and $t_{1u\downarrow}$ states at E_F reported by Yang *et al.*, as it could be removed, in principle, by a small change in the exchange potential.

Our calculations of the spin density show that in both the Fe_9 and the Fe_{15} clusters, the central atom has more minority- than majority-spin electrons, while the outer atoms are dominated by majority spins. The spin densities at the nuclear sites for the Fe_{15} case are, in atomic units,

-0.089 (central atom),

-0.265 (first shell),

-0.395 (second shell).

Moreover, we find considerable anisotropy in the spin-density distribution around the central atom. The minority-spin-dominated region is extended along the (111) directions from the central atom toward the nearest neighbors, and is contracted along the (100) directions. The spin distributions and contact densities obtained here are not in accord with results for bulk iron nor with the results of Ref. 7. We believe that either additional atomic shells must be included, or embedding boundary conditions imposed, if results representative of the bulk in this respect are to be obtained.

IV. CONCLUSIONS

We have completed calculations of energy levels in free Fe_7, Fe_9, and Fe_{15} clusters. An expansion in symmetrized Gaussian orbitals was applied to the Kohn-Sham equations of local-spin-density-functional theory. We find for the Fe_{15} cluster, in agreement with previous MS $X\alpha$ calculations, that there is a very substantial degree of agreement in the overall features of the energy-level distributions between cluster and bulk results. However, we do not find similar agreement in respect to the spatial distribution of the spin density, which implies to us that larger clusters must be considered, or different boundary conditions imposed, in order to obtain results consistent with bulk calculation in this respect.

ACKNOWLEDGMENT

This research was supported in part by the U. S. Army Research Office under Contract No. DAAG29-K-81-0006.

APPENDIX: THE DOUBLING GRID

In our doubling grid, which is intended for cubic geometries, we divide space within the $\frac{1}{48}$th irreducible wedge in several divisions. Space within each division is filled with elementary cubes of the same size. The size of the elementary cubes is made small near atomic centers where some orbital basis functions vary rapidly. The elementary cube size is increased as distances from atomic centers are increased. We could double the elementary cube length for most of the successive divisions except at one stage where approximate doubling was used to avoid an unnecessary explosion in the number of elementary cubes due to the necessity of rapidly increasing number of subdivisions.

The sampling points for integration are chosen to be at the center of each elementary cube even in cases where only part of the cube remains within the wedge. This choice of sampling point is obviously natural for cubes which are completely within the wedge and is also natural for cubes having only portions of their volume within the wedge although it can be seen with simple reasoning that we are wasting sampling points by such a choice. Avoiding high-symmetry planes may be desirable in placing sampling points, but we could not find any other choice of sampling points which could give a better result. For example, we tried shifting our points to center-of-mass positions for fractional cubes (in the full cube it remains at the same position) only to find worse results.

Another point of importance is the necessity of choosing comparable cube sizes for comparable regions of space. If one part of the space were given a finer grid due to some interest in that particular region, the integration result became worse for those cases where proper cancellation could not be obtained due to failure to employ a finer grid in other relevant regions.

The fact that we have a situation where we cannot fill the region with cubes, unless we continue with strict doubling, can be seen with simple reasoning. Consider a two-dimensional grid: In the two-subdivision case, where each doubled-length division is divided into two along the abscissa within its own division, we have found it acceptable to have basic length increasing by

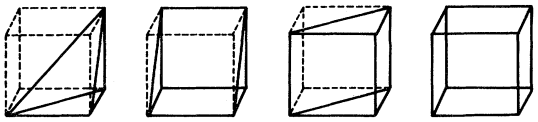

FIG. 6. Figures arising from the partition of cubes by wedge boundaries.

a, $2a$, $3a$, $6a$, $12a$, $24a$, ...

for divisions I, II, III, ..., respectively. If this procedure is not followed, awkwardly shaped fractionally filled regions result.

The accuracy obtainable from a given grid was evaluated by using the grid to compute overlap integrals. Analytic results for these are easy to obtain for comparison purposes. Since the exchange-correlation potential for which the grid is intended is slowly varying, the overlap-integral test should be representative.

In the iron-cluster system, we chose 11 basic doublings for a two subdivision case with minimum cube length of $a=0.000\,44$ a.u., giving a total number of ≈ 1300 points in the Fe_9 system and ≈ 2100 points in the Fe_{15} system. The errors in the overlap test are about 3%. Choosing a four-subdivision case gave better accuracy with four doublings and a minimum cube length of $a=0.0015$ a.u. This generated ≈ 6300 points in the Fe_9 system and yielded about 1% accuracy. Four additional doubling regions were added to the above-mentioned number of basic doubling regions to extend the integration region into the exterior of the cluster. The errors in our overlap test were almost always underestimates of the magnitude of the integrals. This implies that we may slightly underestimate the magnitude of exchange-correlation effects in our calculation.

In the actual implementation of grid generation we filled the space within each division by several typical blocks. Subprograms were made for each typical block in which all grid points as well as weight factors are generated once the choice of subdivision numbers along the abscissa and the data for block dimension lengths and elementary cube length are provided.

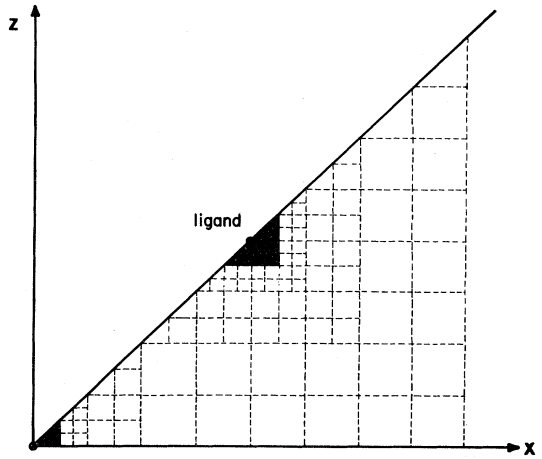

FIG. 7. Two-dimensional cross section of the doubling grid for a one-shell bcc system. The cross-hatched areas are regions of smaller divisions than those explicitly illustrated.

We have found that any elementary region within the wedge takes one of the four shapes shown in Fig. 6. There is no ambiguity in choosing the sampling points for these shapes which obviously are at the center of the cubes, though this will be on a high-symmetry plane in some cases. This, in effect, reduces the number of independent sampling points as a result.

A two-dimensional cross section of a two-subdivision case is sketched in Fig. 7 (this could be either the bcc or fcc first-neighbor situation). Additional discussion and programs for the construction of this grid are found in Ref. 6.

[1]B. Delley and D. E. Ellis, J. Chem. Phys. **76**, 1949 (1982).
[2]W. Kohn and L. J. Sham, Phys. Rev. **140**, A1133 (1965).
[3]C. S. Wang and J. Callaway, Comput. Phys. Commun. **14**, 327 (1978).
[4]H. Sambe and R. H. Felton, J. Chem. Phys. **62**, 1122 (1975).
[5]J. W. Mintmire and B. W. Dunlap, Phys. Rev. A **25**, 88 (1983).
[6]K. Lee, Ph.D. thesis, Louisiana State University, 1984, available from University Microfilms International, Ann Arbor, Michigan 48106.
[7]C. Y. Yang, K. H. Johnson, D. R. Salahub, J. Kaspar, and R. P. Messmer, Phys. Rev. B **24**, 5673 (1981).
[8]U. von Barth and L. Hedin, J. Phys. C **5**, 1629 (1972).
[9]A. K. Rajagopal, S. P. Singhal, and J. Kimball (unpublished), as quoted by A. K. Rajagopal, in *Advances in Chemical Physics*, edited by G. I. Prigogine and S. A. Rice (Wiley, New York, 1979), Vol. 41, p. 59.
[10]A. J. H. Wachters, J. Chem. Phys. **52**, 1033 (1970).
[11]B. I. Dunlap, Phys. Rev. A **25**, 2847 (1982).
[12]P. H. Dederichs and R. Zeller, Phys. Rev. B **28**, 5462 (1983).
[13]E. A. Rohlfing, D. M. Cox, and A. Kaldor, Chem. Phys. Lett. **99**, 161 (1983).
[14]J. C. Slater, *The Self-Consistent Field for Molecules and Solids* (McGraw-Hill, New York, 1974).
[15]J. Callaway and C. S. Wang, Phys. Rev. **16**, 2095 (1977).
[16]V. Heine, in *Solid State Physics*, edited by H. Ehrenreich, F. Seitz, and D. Turnbull (Academic, New York, 1980), Vol. 35, p. 1.